

LETTER • OPEN ACCESS

Experimental realization of a hybrid trapped field magnet lens using a GdBaCuO magnetic lens and MgB₂ bulk cylinder

To cite this article: Sora Namba *et al* 2019 *Supercond. Sci. Technol.* **32** 12LT03

View the [article online](#) for updates and enhancements.



IOP | ebooks™

Bringing you innovative digital publishing with leading voices to create your essential collection of books in STEM research.

Start exploring the collection - download the first chapter of every title for free.

Letter

Experimental realization of a hybrid trapped field magnet lens using a GdBaCuO magnetic lens and MgB₂ bulk cylinder

Sora Namba^{1,3}, Hiroyuki Fujishiro¹, Tomoyuki Naito¹,
Mark D Ainslie² and Keita Takahashi¹

¹Department of Physical Science and Materials Engineering, Faculty of Science and Engineering, Iwate University, 4-3-5 Ueda, Morioka 020-8551, Japan

²Department of Engineering, University of Cambridge, Trumpington Street, Cambridge CB2 1PZ, United Kingdom

E-mail: g0318128@iwate-u.ac.jp

Received 13 August 2019, revised 13 October 2019

Accepted for publication 18 October 2019

Published 5 November 2019



CrossMark

Abstract

A hybrid trapped field magnet lens (HTFML) is a promising device that is able to concentrate a magnetic field higher than the applied field continuously, even after removing an external field, which was conceptually proposed by the authors in 2018. This paper presents, for the first time, the experimental realization of the HTFML using a GdBaCuO magnetic lens and MgB₂ trapped field magnet cylinder. A maximum concentrated magnetic field of $B_c = 3.55$ T was achieved at the central bore of the HTFML after removing an applied field of $B_{app} = 2.0$ T at $T = 20$ K. For higher B_{app} , the B_c value was not enhanced because of a weakened lens effect due to magnetic flux penetration into the bulk GdBaCuO material comprising the lens. The enhancement of the trapped field using such an HTFML for the present experimental setup is discussed in detail.

Keywords: hybrid trapped magnet field lens, bulk superconductors, trapped field magnets, magnetic lens, vortex pinning effect, magnetic shielding effect

(Some figures may appear in colour only in the online journal)

1. Introduction

Trapped field magnets (TFMs) using superconducting bulks such as REBaCuO (RE: a rare earth element or Y) and MgB₂ have been vigorously investigated for various practical applications; for example, rotating machines, magnetic separation, flywheel energy storage systems and so on [1–3]. Superconducting bulk TFMs, in which magnetic flux is

trapped by the strong ‘vortex pinning effect’, are usually magnetized by field-cooled magnetization (FCM) using a high, stationary magnetic field, for which a magnetic field nearly the same or slightly lower than the applied field can be trapped. The trapped field capability of such bulks, as estimated from state-of-the-art $J_c(B, T)$ characteristics could exceed 20 T at 20 K in a disk bulk pair [4]. However, the trapped field is limited experimentally by the poor mechanical strength of the brittle ceramic material [5]. A large Lorentz force is developed in the bulk during the magnetization process, which sometimes results in crack formation and propagation, leading to eventual mechanical failure [6, 7]. To date, REBaCuO disk bulks have trapped magnetic fields over 17 T by mechanical reinforcement using glass fiber reinforced epoxy resin or shrink-fit stainless steel to reduce the

³ Author to whom any correspondence should be addressed



Original content from this work may be used under the terms of the Creative Commons Attribution 3.0 licence. Any further distribution of this work must maintain attribution to the author(s) and the title of the work, journal citation and DOI.

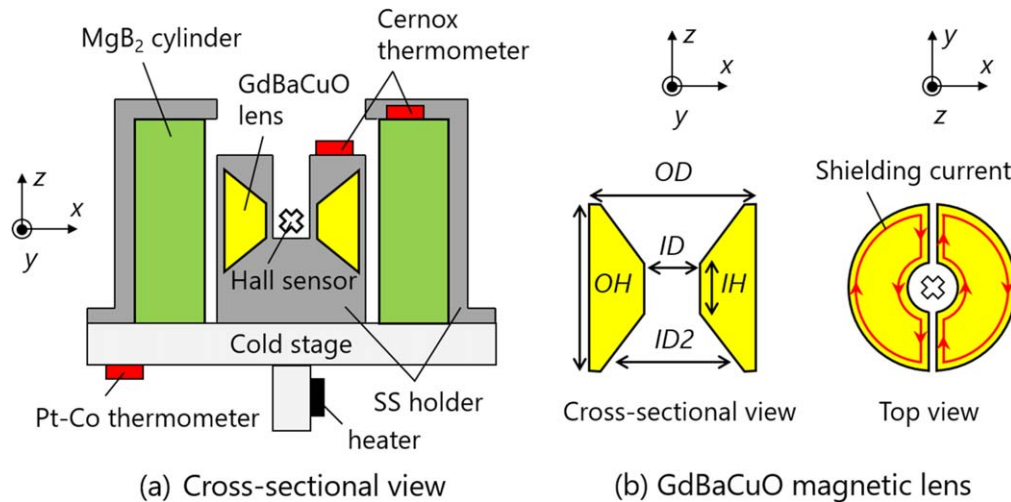


Figure 1. (a) Cross-sectional view of the schematic illustration of the experimental setup for the HTFML on the cold stage of a refrigerator. (b) Cross-sectional and top views of the GdBaCuO magnetic lens with slits. When a magnetic field is applied along the $+z$ -axis direction to the GdBaCuO magnetic lens, the magnetic field penetrates from the slits and the shielding current flows as shown by the red arrows. As a result, the magnetic field increases along the $+z$ -direction due to the shielding current.

electromagnetic hoop stress [4, 8]. A ring-shaped bulk superconductor that can produce uniform, high magnetic fields within the central bore is a strong candidate for compact cryogen-free nuclear magnetic resonance (NMR) and magnetic resonance imaging (MRI) systems [9–11]. The ^1H spectra of toluene with a full width at half maximum of 0.4 ppm (80 Hz) was achieved in the 10 mm room temperature bore in the bulk NMR [10]. The first MRIs using annular EuBaCuO bulks were also reported with a magnetic homogeneity of 37 ppm (peak-to-peak) achieved in a Φ 6.2 mm \times 9.1 mm cylindrical space with first order shimming [11]. Using this system, a clear 3D image of a chemically-fixed mouse fetus was acquired.

On the other hand, a ‘magnetic lens’ using cone-shaped superconducting bulks has been investigated, in which a magnetic field is concentrated in the bore of the lens using the ‘diamagnetic shielding effect’ of superconducting materials and the available magnetic field in the lens is higher than the applied field generated by an external magnetizing coil [12–18]. For example, a concentrated field of $B_c = 12.42$ T has been achieved at 20 K for a background field of $B_{\text{app}} = 8$ T using a bulk GdBaCuO magnetic lens [12]. Since the magnetic lens effect vanishes after the applied field decreased to zero, the external magnet must be operated continuously, which consumes energy and is not environmentally friendly.

We recently proposed a new concept of a hybrid trapped field magnet lens (HTFML) [19], consisting of a cylindrical bulk TFM exploiting the ‘vortex pinning effect’, combined with a bulk magnetic lens exploiting the ‘diamagnetic shielding effect’. Using numerical simulations, the HTFML was shown to be able to reliably generate a magnetic field in the central bore of the magnetic lens that is higher than both the trapped field in the single cylindrical bulk TFM and the external magnetizing field, even after the externally applied field decreases to zero. For a REBaCuO magnetic lens and MgB₂ TFM cylinder, the HTFML could reliably generate a

concentrated magnetic field of $B_c = 4.73$ T with an external magnetizing field $B_{\text{app}} = 3$ T. For an HTFML comprised of REBaCuO bulks for both magnetic lens and TFM cylinder, a concentrated magnetic field of $B_c = 13.49$ T could be generated with an external magnetizing field $B_{\text{app}} = 10$ T, where the temperature of both parts is controlled independently [19]. In addition, the shape of the magnetic lens in the HTFML has been optimized, and the mechanical stress in the cylinder and lens parts has also been estimated during the magnetizing process [20].

In this paper, we present, for the first time, the experimental realization of the HTFML using a GdBaCuO magnetic lens and MgB₂ TFM cylinder, based on the same magnetizing procedure proposed in [19]. The experimental results are compared with the simulated ones and enhancement of the B_c value in HTFML is discussed in detail.

2. Experimental procedure

2.1. Experimental setup

Figure 1(a) shows the schematic cross-section of the experimental setup of the HTFML on the cold stage of a refrigerator. The MgB₂ cylindrical bulk (60 mm in outer diameter (OD), 40 mm in inner diameter (ID), and 60 mm in height (H)) was fabricated using the infiltration method by Experiments Projects Constructions S. R. I., Italy [21, 22]. Figure 1(b) shows the cross-section and top view of the GdBaCuO magnetic lens. The GdBaCuO magnetic lens was prepared by the following process: stacked GdBaCuO cylindrical bulks (OD = 36 mm, ID = 10 mm, H = 30 mm), fabricated using the QMGTM method by Nippon Steel Corporation, Japan [23, 24], were machined into a cone-shape of OD = 30 mm, ID = 10 mm, ID2 = 26 mm, outer height (OH) = 30 mm and inner height (IH) = 8.0 mm, as shown in figure 1(b). The dimensions of the bulk magnetic lens were

optimized using numerical simulations [20]. Thin slits of width $200\ \mu\text{m}$ was made to disrupt the circumferential flow of the shielding current during the zero-field-cooling (ZFC) process, which plays an important role in magnetic flux concentration for the magnetic lens [19]. When an external magnetic field is applied along the $+z$ -axis direction to the GdBaCuO magnetic lens, the same magnetic field penetrates into the central bore from the slits. The shielding current flows as shown by the red arrows in figure 1(b) and an additional magnetic field exists along the $+z$ -axis direction, mainly due to the counterclockwise shielding current nearest to the central bore. As a result, the magnetic field is enhanced along the $+z$ -axis direction, which is then higher than the applied field.

The GdBaCuO magnetic lens was encapsulated in a stainless steel (SS) holder to prevent fracture of the bulk due to the large Lorentz force during the magnetization process, and was connected thermally to the cold stage of the refrigerator. The MgB_2 cylindrical bulk was reinforced by a SS cylinder (ID = 60 mm, OD = 66 mm and $H = 60$ mm) and the top SS plate (ID = 36 mm, OD = 66 mm and $H = 3$ mm), which were effective in preventing mechanical fracture [25, 26]. These SS holders apply a compressive stress to the bulk cylinder and bulk lens during the cooling process from room temperature to the operating temperature (e.g. 20 K) due to the difference in the coefficient of thermal expansion between SS and the bulk superconducting materials. Two CERNOX™ thermometers were attached for monitoring the temperature of the HTFML; one was mounted directly on the top surface of the MgB_2 cylinder, and the other was placed on the top surface of the SS holder of the GdBaCuO lens. Thin indium sheets were inserted between the bulks and the cold stage of the refrigerator (or SS holder) to obtain good thermal contact. The temperature of the cold stage was controlled using a Pt-Co thermometer and a resistive heater, attached to bottom surface of the cold stage. The concentrated field, B_c , was measured in the central bore of the HTFML by an axial-type Hall sensor (F W Bell, BHA-921). The HTFML device was placed in a vacuum chamber and then evacuated by a vacuum pump system.

2.2. Magnetization procedure

Figure 2 shows the time sequence of the external field (left vertical axis), B_{ex} , at the center of the HTFML and the operating temperature (right vertical axis), T , during the magnetizing process of the HTFML. The magnetizing external field, B_{app} , corresponds to the maximum value of B_{ex} . The HTFML device set in the vacuum chamber was inserted into a cryocooled 10 T superconducting solenoid magnet (JASTEC JMTD-10T100). First, the MgB_2 bulk cylinder and GdBaCuO bulk lens were cooled to $T = 40$ K. In this stage, the MgB_2 cylinder is in the normal state and the GdBaCuO lens is in the superconducting state, where the time step (TS) is defined as $TS = 0$. The proof-of-concept experiments of the HTFML were performed according to the following magnetizing process.

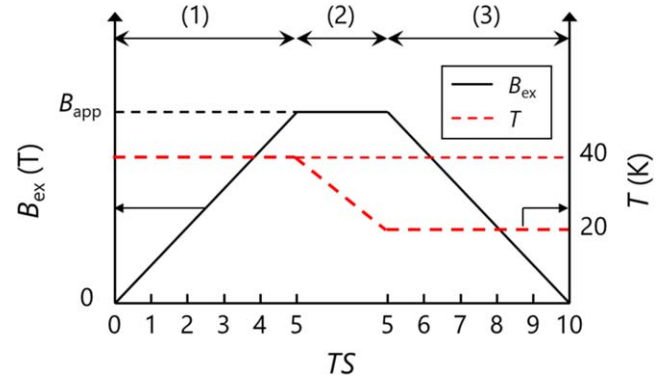


Figure 2. Time step (TS) sequence of the external field (black: left vertical axis), B_{ex} , at the center of the HTFML and the operating temperature (red: right vertical axis), T , during the magnetizing process to realize the HTFML. The magnetizing applied field, B_{app} , corresponds to the maximum value of B_{ex} .

- (1) The external magnetic field, B_{ex} , was ramped up linearly at $+0.222\ \text{T min}^{-1}$ to $B_{\text{app}} = 1\text{--}3\ \text{T}$ over five steps, where TS of the ascending stage is defined as $TS = 1\text{--}5$. This process corresponds to ZFC magnetization of the GdBaCuO lens, in which the magnetic field at the center is essentially higher than B_{app} because of the shielding effect by the magnetic lens.
- (2) The temperatures of both the MgB_2 cylinder and GdBaCuO lens were decreased to $T = 20\ \text{K}$ under the applied field B_{app} , with both materials now in the superconducting state.
- (3) B_{ex} was decreased linearly at $-0.011\ \text{T min}^{-1}$ over five steps ($TS = 6\text{--}10$) down to zero. During this process, the MgB_2 cylinder was magnetized by FCM and magnetic flux was trapped in the cylinder. A magnetic field at the center of the magnetic lens still remains due to the existence of the trapped field in the MgB_2 cylinder. As a result, the HTFML can reliably generate a magnetic field higher than the trapped field in the single MgB_2 TFM cylinder and B_{app} , even after $B_{\text{ex}} = 0$.

Prior to the HTFML experiments, the trapped field properties of the MgB_2 cylinder and the magnetic concentration capability of the GdBaCuO lens were investigated independently using the same time sequence as shown in figure 2 under the external magnetic field of $B_{\text{app}} = 1\text{--}3\ \text{T}$, in which either the MgB_2 cylinder or GdBaCuO lens was set on the cold stage.

3. Results and discussion

3.1. Trapped field capability of the single MgB_2 cylinder

To confirm the trapped field capability of MgB_2 cylinder, the trapped field properties of the single MgB_2 cylinder was measured. Figure 3(a) shows the time evolution of the external field, B_{ex} , and trapped field, B_c , at the center of the single MgB_2 cylinder during the same time sequence shown

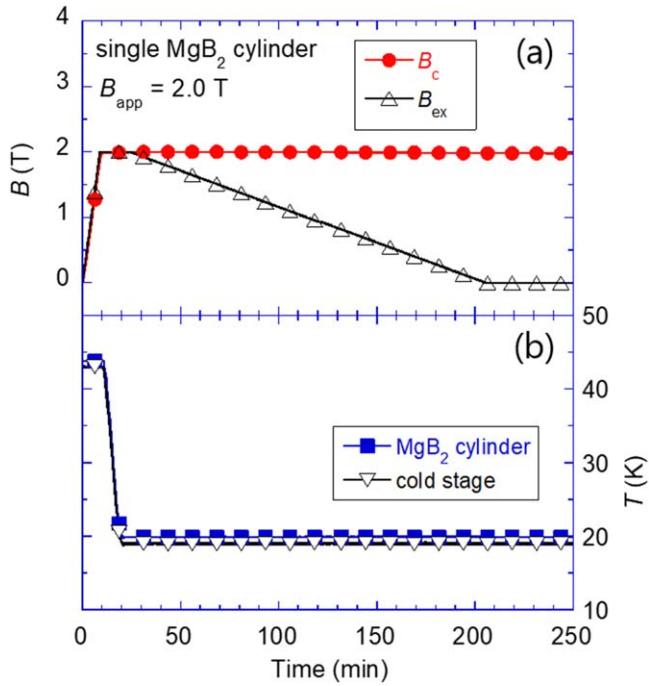


Figure 3. Time evolution of (a) the measured magnetic field, B_c , at the center of the single MgB_2 cylinder and external field, B_{ex} , and (b) the temperatures of MgB_2 cylinder and cold stage during the magnetization process for an applied field of $B_{app} = 2.0$ T.

in figure 2 under an external magnetic field of $B_{app} = 2.0$ T. Figure 3(b) shows the time evolution of the temperatures of the cold stage and the MgB_2 cylinder for the same process. In the ascending stage, the magnetic field, B_c , increased linearly with increasing B_{ex} and the magnitude of B_c was the same as the external field ($B_c = B_{ex} = 2.0$ T) because the MgB_2 cylinder was in normal state ($T = 40$ K). In the descending stage, after cooling to 20 K, the B_{ex} was slowly decreased at a constant rate of -0.011 T min^{-1} and the FCM process was performed for the MgB_2 cylinder. As a result, a trapped field remained of $B_c = 2.0$ T after B_{ex} was decreased to zero due to the conventional vortex pinning effect. In figure 3(b), the temperature of the MgB_2 cylinder was nearly the same as that of the cold stage because of the good thermal contact.

Figure 4 shows the TS dependence of the trapped field, B_c , at the center of the single MgB_2 cylinder under external magnetic fields of $B_{app} = 1-3$ T. In the ascending stage from $TS = 0$ to 5, the magnetic field increases linearly with increasing TS and the magnitude is the same as the external field because the MgB_2 cylinder is in normal state. In the descending stage of the FCM process, for the applied fields of $B_{app} = 1.0$ and 2.0 T, trapped fields of 1.00 T and 1.98 T, respectively, were achieved at $TS = 10$ without flux creep. On the other hand, for higher applied fields of 2.5 and 3.0 T, the TS dependence of B_c after $TS = 5$ gradually decreased and the final trapped field was 2.18 T, which suggests the maximum trapped field capability of the MgB_2 cylinder at $T = 20$ K. The trapped field cannot increase over 2.18 T, even if applied field is higher than 3.0 T. In the conceptual paper [19], $B_c = 2.85$ T was predicted at the final step at $T = 20$ K in the bore of MgB_2 cylinder for $B_{app} = 3.09$ T. The lower B_c

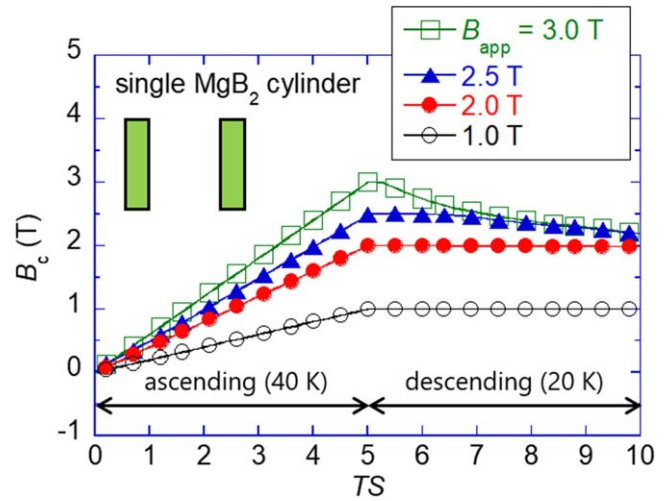


Figure 4. Time step (TS) dependence of the measured magnetic field, B_c , at the center of the single MgB_2 cylinder during the magnetization process for applied fields $B_{app} = 1.0-3.0$ T.

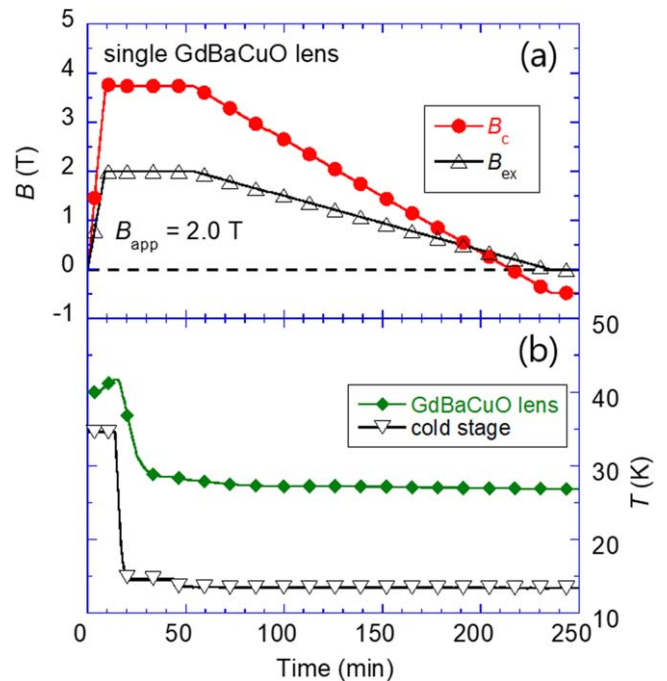


Figure 5. Time evolution of (a) the measured magnetic field, B_c , at the center of the single GdBaCuO bulk lens and external field, B_{ex} , and (b) the temperatures of GdBaCuO bulk lens and cold stage during the magnetization process for an applied field of $B_{app} = 2.0$ T.

value in the present experiment results from the lower $J_c(B, T)$ of the present MgB_2 cylinder, compared with that used in the simulations in [19].

3.2. Magnetic shielding capability of the single GdBaCuO bulk lens

The magnetic shielding capability of the GdBaCuO bulk lens was measured using the single GdBaCuO bulk lens during the ZFC process. Figure 5(a) shows the time evolution of the magnetic field, B_c , at the center of the single GdBaCuO bulk

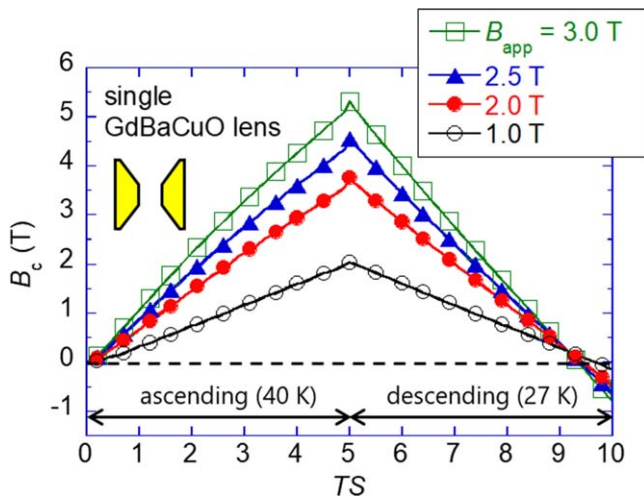


Figure 6. TS dependence of the measured magnetic field, B_c , at the center of the single GdBaCuO magnetic lens during the magnetization process under applied fields, $B_{app} = 1.0\text{--}3.0\text{ T}$. For $TS = 10$, the B_c value increased negatively with increasing B_{app} .

lens and the external field, B_{ex} , during the same time sequence shown in figure 2, under an external magnetic field of $B_{app} = 2.0\text{ T}$. Figure 5(b) shows the time evolution of the temperatures of GdBaCuO bulk lens and the cold stage under the same process. In the ascending stage, a clear magnetic field concentration was observed; $B_c = 3.76\text{ T}$ was achieved, which resulted in a magnetic field concentration ratio of $B_c/B_{app} = 1.88$. A temperature rise of about 2.1 K took place during ascending stage from 0 to 10 min, originating from magnetic flux penetration into the magnetic lens. When the temperature of the cold stage was set to 20 K, the minimum temperature of the GdBaCuO bulk lens encapsulated by the SS holder was only 26.5 K, which may come from an imperfect thermal contact between the bulk lens and the SS holder. It should be noted that the final B_c value was not zero, but a negative one of -0.48 T . This result suggests that some magnetic flux penetrated into the surface of the bulk lens and a residual magnetic field along the $-z$ -direction existed due to the vortex pinning effect.

Figure 6 shows the TS dependence of the magnetic field, B_c , at the center of the single GdBaCuO bulk lens during the ZFC process under applied magnetic fields of $B_{app} = 1.0\text{--}3.0\text{ T}$. In the ascending stage from $TS = 0$ to 5, the magnetic field was concentrated by the shielding current. For lower $B_{app} = 1$ and 2 T, $B_c = 2.04$ and 3.76 were achieved at $TS = 5$, which correspond to magnetic field concentration ratios, B_c/B_{app} , of 2.04 and 1.88, respectively. The B_c values increased for higher B_{app} , which were 4.55 T and 5.19 T for $B_{app} = 2.5$ and 3.0 T at $TS = 5$, respectively. However, the magnetic field concentration ratio, B_c/B_{app} , gradually decreased due to increased magnetic flux penetration into the bulk lens. For the final stage ($TS = 10$), at which the external field was zero, the B_c value increased negatively with increasing B_{app} for the same reason. For all the cases, the minimum temperature of the GdBaCuO bulk lens encapsulated by the SS holder was only 26.5 K. To improve the

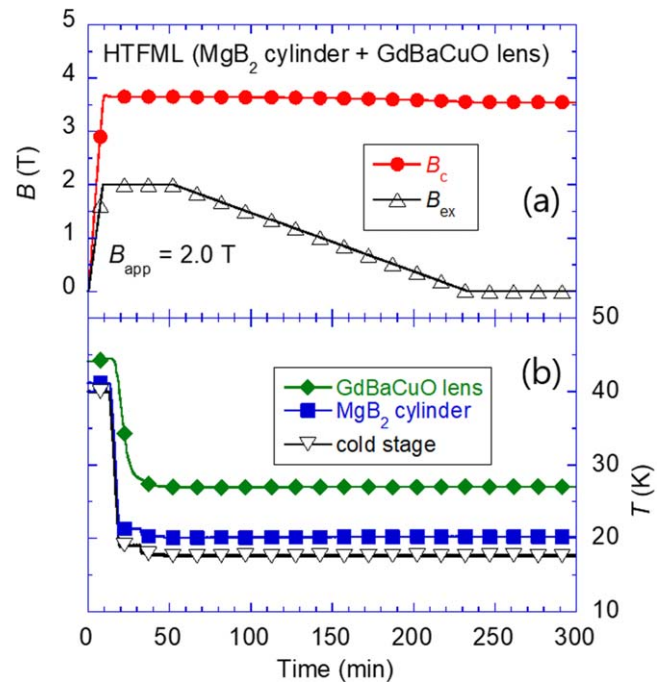


Figure 7. Time evolution of (a) the measured magnetic field, B_c , at the center of the HTFML and external field, B_{ex} , and (b) the temperatures for each measurement point during the magnetizing process for $B_{app} = 2.0\text{ T}$.

performance of the magnetic lens, lowering its temperature is necessary.

3.3. Realization of the HTFML

Finally, we present the experimental realization of the HTFML using GdBaCuO magnetic lens, combined with the MgB_2 bulk cylinder. Figure 7(a) shows the time evolution of the magnetic field, B_c , at the center of the HTFML during the magnetizing process shown in figure 2 under an external magnetic field of $B_{app} = 2.0\text{ T}$. Figure 7(b) shows the time evolution of the temperatures measured at each position. In the ascending stage, the B_c value reached 3.65 T and then slightly decreased to 3.55 T at the end of the descending stage due to flux flow. The magnetic field concentration ratio, B_c/B_{app} , was 1.76 at the end of the ramp. The temperatures of the MgB_2 cylinder and the GdBaCuO bulk lens on the SS holder were 20.0 and 26.5 K, respectively. These results demonstrate the HTFML effect experimentally for the first time.

Figure 8 shows the TS dependence of the magnetic field, B_c , at the center of the HTFML during the magnetizing process under applied fields of $B_{app} = 1.0\text{--}3.0\text{ T}$. At the end of the ascending stage ($TS = 5$), the B_c value for each B_{app} was nearly the same as that for the single GdBaCuO magnetic lens case, as shown in figure 6. In the descending stage, for $B_{app} = 1.0$ and 2.0 T, the B_c value was nearly the same as that at $TS = 5$. On the other hand, for $B_{app} = 2.5$ and 3.0 T, the B_c value gradually decreases with increasing TS. As a result, the final B_c value for $B_{app} = 2.5$ and 3.0 T was smaller than that for $B_{app} = 2.0\text{ T}$. The concentrated magnetic field, B_c , at

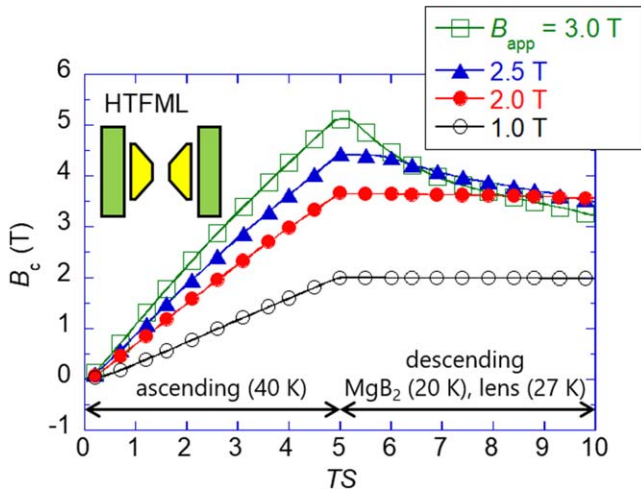


Figure 8. TS dependence of the measured magnetic field, B_c , at the center of the HTFML device during the magnetization process under various applied fields, $B_{app} = 1.0\text{--}3.0\text{ T}$.

Table 1. Concentrated magnetic field, B_c , at TS = 5 and 10 at the center of the HTFML, and calculated magnetic field concentration ratio, B_c/B_{app} for various applied magnetic fields, B_{app} .

B_{app} (T)	B_c (T) at TS = 5	B_c (T) at TS = 10	B_c/B_{app} at TS = 10
1.0	2.00	1.99	1.99
2.0	3.65	3.55	1.76
2.5	4.45	3.46	1.38
3.0	5.19	3.22	1.07

TS = 5 and 10 at the center of the HTFML, and calculated magnetic field concentration ratio, B_c/B_{app} , for the various applied magnetic fields, B_{app} , are summarized in table 1. A maximum B_c value of 3.55 T was achieved for $B_{app} = 2.0\text{ T}$.

In the concept paper, in which the HTFML was proposed to be constructed using a REBaCuO magnetic lens and MgB₂ TFM cylinder, a concentrated magnetic field $B_c = 4.73\text{ T}$ was predicted for an external magnetizing field $B_{app} = 3\text{ T}$ using numerical simulations [19]. However, the maximum B_c value was as low as 3.55 T experimentally under the same magnetizing process for $B_{app} = 2.0\text{ T}$. This difference occurs for the following reasons. Firstly, the assumed $J_c(B, T)$ characteristics of the MgB₂ and GdBaCuO bulks used in the simulations were higher than those of the actual bulks used in the experiments. Secondly, the minimum temperature of the GdBaCuO bulk lens was only 26.5 K, when the temperature of the cold stage was set to 20.0 K. To enhance the HTFML effect for the present MgB₂ cylinder and GdBaCuO bulk lens, the thermal contact between the GdBaCuO bulk lens and the SS holder must be improved. Nevertheless, we have realized the HTFML effect experimentally for the first time. Our final goal is to build and test an HTFML using a GdBaCuO cylinder and GdBaCuO lens, for which a B_c value in excess of 10 T (e.g. $B_c = 13.5\text{ T}$ [19]) is predicted for a magnetizing process with $B_{app} = 10\text{ T}$. A cryocooled 10 T superconducting solenoid magnet with a large room temperature

bore (e.g. 100 mm in ID) has become more readily available in the science and engineering research communities outside of the field of superconductivity. Thus, building on these findings, we aim to provide easily a concentrated magnetic field higher than 10 T in an open space using this HTFML system.

4. Conclusion

We have presented, for the first time, the experimental realization of a HTFML, based on the device design and magnetizing procedure recently proposed in [19, 20]. The important results and conclusions in this study are summarized as follows.

- (1) The HTFML effect was demonstrated experimentally using GdBaCuO magnetic lens and MgB₂ TFM cylinder for the first time, such that a magnetic field can be generated in the central bore of the magnetic lens that is higher than both the trapped field in the single cylindrical bulk TFM and the external magnetizing field, even after the externally applied field decreases to zero.
- (2) A maximum concentrated magnetic field of $B_c = 3.55\text{ T}$ was achieved in the central bore of the HTFML device after removing an applied field of $B_{app} = 2.0\text{ T}$ at $T = 20\text{ K}$. The maximum B_c value was smaller than the one estimated by numerical simulations, which results from the lower $J_c(B, T)$ and higher operating temperature, compared with those of the numerical predictions.
- (3) For higher B_{app} , the B_c value was not enhanced because of a weakened lens effect due to magnetic flux penetration into the bulk GdBaCuO material comprising the lens. To enhance the HTFML effect, improving the thermal contact between the HTFML and the cold stage and lowering temperature of the GdBaCuO lens and MgB₂ TFM cylinder is necessary for the present setup.

Acknowledgments

The authors thank Mr Y Yanagi of IMRA Material R&D Co., Ltd, Japan, and Dr G Giunchi of Materials Science Consultant, Italy, for their valuable experimental supports. This research is supported by Adaptable and Seamless Technology transfer Program through Target-driven R&D (A-STEP) from Japan Science and Technology Agency (JST), Grant No. VP30218088419 and by JSPS KAKENHI Grant No. 19K05240. M D Ainslie would like to acknowledge financial support from an Engineering and Physical Sciences Research Council (EPSRC) Early Career Fellowship, EP/P020313/1. All data are provided in full in the results section of this paper.

ORCID iDsSora Namba  <https://orcid.org/0000-0001-7268-5326>Hiroyuki Fujishiro  <https://orcid.org/0000-0003-1483-835X>Tomoyuki Naito  <https://orcid.org/0000-0001-7594-3466>Mark D Ainslie  <https://orcid.org/0000-0003-0466-3680>Keita Takahashi  <https://orcid.org/0000-0002-8278-2688>**References**

- [1] Zhou D, Izumi M, Miki M, Felder B, Ida T and Kitano M 2012 *Supercond. Sci. Technol.* **25** 103001
- [2] Hayashi H, Tsutsumi K, Saho N, Nishijima N and Asano K 2003 *Physica C* **392–396** 745–8
- [3] Werfel F N, Floegel-Delor U, Rothfeld R, Riedel T, Goebel B, Wippich D and Schirrmeister P 2012 *Supercond. Sci. Technol.* **25** 014007
- [4] Tomita M and Murakami M 2003 *Nature* **421** 517–20.
- [5] Sakai N, Seo S-J, Inoue K, Miyamoto T and Murakami M 2000 *Physica C* **335** 107–11
- [6] Ren Y, Weinstein R, Liu J, Sawh R P and Foster C 1995 *Physica C* **251** 15–26
- [7] Fuchs G, Schätzle P, Krabbes G, Gruß S, Verges P, Müller K-H, Fink J and Schultz L 2000 *Appl. Phys. Lett.* **76** 2107–9
- [8] Durrell J H *et al* 2014 *Supercond. Sci. Technol.* **27** 082001
- [9] Nakamura T, Itoh Y, Yoshikawa M, Oka T and Uzawa J 2007 *Concepts Magn. Reson. B* **31B** 65–70
- [10] Nakamura T, Tamada D, Yanagi Y, Itoh Y, Nemoto T, Utumi H and Kose K 2015 *J. Magn. Reson.* **259** 68–75
- [11] Ogawa K, Nakamura T, Terada Y, Kose K and Haishi T 2011 *Appl. Phys. Lett.* **98** 234101
- [12] Zhang Z Y, Matsumoto S, Teranishi R and Kiyoshi T 2012 *Supercond. Sci. Technol.* **25** 115012
- [13] Choi S, Yoon J-H, Lee B-S, Won M-S, Ok J-W, Zhang Z-Y, Kiyoshi T, Matsumoto S and Lee S-H 2012 *J. Appl. Phys.* **111** 07E728
- [14] Kiyoshi T, Choi S, Matsumoto S, Asano T and Uglietti D 2009 *IEEE Trans. Appl. Supercond.* **19** 2174–7
- [15] Zhang Z Y, Matsumoto S, Teranishi R and Kiyoshi T 2013 *Supercond. Sci. Technol.* **26** 045001
- [16] Asano T, Itoh K, Matsumoto S, Kiyoshi T, Wada H and Kido G 2005 *IEEE Trans. Appl. Supercond.* **15** 3157–60
- [17] Choi S, Kiyoshi T and Matsumoto S 2009 *J. Appl. Phys.* **105** 07E705
- [18] Miyazoe A, Nakagawa R, Hori C, Tanaka H and Imamura Y 2018 *IEEE Trans. Appl. Supercond.* **28** 4700205
- [19] Takahashi K, Fujishiro H and Ainslie M D 2018 *Supercond. Sci. Technol.* **31** 044005
- [20] Namba S *et al* 2019 *IEEE Trans. Appl. Supercond.* **29** 6801605
- [21] Giunchi G, Raineri S, Wesche R and Bruzzone P L 2004 *Physica C* **401** 310–5
- [22] Giunchi G, Ripamonti G, Cavallin T and Bassani E 2016 *Cryogenics* **46** 237–42
- [23] Morita M, Sawamura M, Takebayashi S, Kimura K, Teshima H, Tanaka M, Miyamoto K and Hashimoto M 1994 *Physica C* **235–240** 209–12
- [24] Nariki S, Teshima H and Morita M 2016 *Supercond. Sci. Technol.* **29** 034002
- [25] Fujishiro H, Takahashi K, Naito T, Yanagi Y, Itoh Y and Nakamura T 2018 *Physica C* **550** 52–6
- [26] Fujishiro H, Naito T, Yanagi Y, Itoh Y and Nakamura T 2019 *Supercond. Sci. Technol.* **32** 065001